COMPUTATIONAL FLUID DYNAMICS BENCHMARK USING AP1000®
¼-SCALE UPPER HEAD TEST DATA

William L. Moody, Teresa A. Bissett, Yiban Xu, and Gregory A. Meyer
The Westinghouse Electric Company LLC
1000 Westinghouse Drive, Cranberry Township, PA 16066, USA
moodywl@westinghouse.com; bissetta@westinghouse.com; xuy@westinghouse.com; meyerga@westinghouse.com

ABSTRACT

A computational fluid dynamics (CFD) analysis, benchmark and uncertainty program was carried out by the Westinghouse Electric Company LLC on the upper head of the reactor vessel internals (RVI) of the AP1000® plant. CFD was used to determine velocity in the upper head due to the complex nature of the flow field, which includes phenomena such as jetting, recirculation, and cross-flow/shear flow over complex structures. The objective for this analysis was to predict the velocity field near the periphery components and validate the results. Velocities from this analysis were used as input to upper head component American Society of Mechanical Engineers (ASME) structural code evaluations.

The CFD model was developed in Star-CCM+. Based on previous experience of flow fields of this nature, a trim-cell hexahedral mesh was used because of its appropriate resolution and efficient development times. An unsteady RANS approach was employed, due to the expected unsteady nature of the flow field. An uncertainty analysis was performed on the CFD results, closely following the approach outlined in the ASME Verification and Validation (V&V) 20 [1]. This includes mesh sensitivity analysis, input sensitivity, and turbulence model sensitivity. The numerical uncertainty was assessed by using the least squares approach because monotonic grid convergence was not observed. Extrapolation to prototypic scale, though not covered in [1], was performed in this work since benchmark testing was conducted at scaled dimensions and a reduced Reynolds number.

Testing was conducted at the Applied Research Laboratory (ARL) of the Pennsylvania State University in order to benchmark the CFD results. The test design was a scale model representation of the AP1000 upper head RVI, and geometric similitude was preserved. Velocity measurements were taken via particle image velocimetry (PIV) and laser Doppler velocimetry (LDV), while volumetric flow rates were monitored using turbine meters. Uncertainty analyses were performed on the test data for inclusion in the comparisons between the test data and CFD results. Contour plots were used for qualitative assessment, while velocity magnitude and direction were used for quantitative assessment of the CFD to test differences. The CFD results compared well with the test data, with a general trend of slightly over predicting the test data. The benchmark results indicate that the CFD model approach appropriately models the complex PWR reactor upper head velocity field needed for structural design qualification inputs. The focus of this paper is on the CFD methodology and uncertainty analyses.

KEYWORDS
CFD Benchmark, Unsteady RANS, Uncertainty analysis, Scale model test

1. INTRODUCTION

The AP1000® PWR reactor vessel upper head region consists of a plenum with numerous internal components consisting of tubes, rods and plates of complex geometries. Cooling flow to the upper head is supplied by nozzles (UHCN) located at the top of the RVI downcomer annulus region. A CFD model was used to determine velocity in the upper head due to the complex nature of the flow field, which includes phenomena such as jetting, recirculation, and cross-flow/shear flow over complex structures. The objective for the full-scale CFD analysis was to predict the velocity field near the periphery components and validate the results at prototypic conditions. Velocity fields from this analysis were used as input to the American Society of Mechanical Engineers (ASME) structural code evaluations. In order to benchmark the CFD model, a validation effort was successfully conducted using V&V analysis methods outlined in [1], including validation using relevant test results.

This paper presents the computational fluid dynamics (CFD) benchmark efforts relative to a ¼ scale AP1000 upper head flow test. A ¼ scale model test of the AP1000® reactor vessel upper head region was performed at the Pennsylvania State University/Applied Research Laboratory (ARL). The scale model test was performed because of the impractical nature of obtaining velocities at full-scale prototypic conditions. For benchmarking purposes, the comparisons were made to local velocity components in the test. The local velocity components were compared quantitatively at points, as well as qualitatively with velocity vector contours. An uncertainty analysis (discretization, input, etc.) was performed based on various sensitivity runs in accordance with [1] and also included an assessment of the uncertainty in scaling from the ¼ scale test to full scale.

The geometry for the test was created using scaled prototypic design drawings. All general geometry details in the test were modeled in the CFD model, with the exception of small insignificant features (e.g., small bolt heads). Also, due to known geometric symmetries, the benchmark test was built as a 90° sector, as opposed to the full 360°. The uncertainty due to this simplification is included in the overall validation uncertainty analysis. A representation of the geometry can be seen in Figure 1.

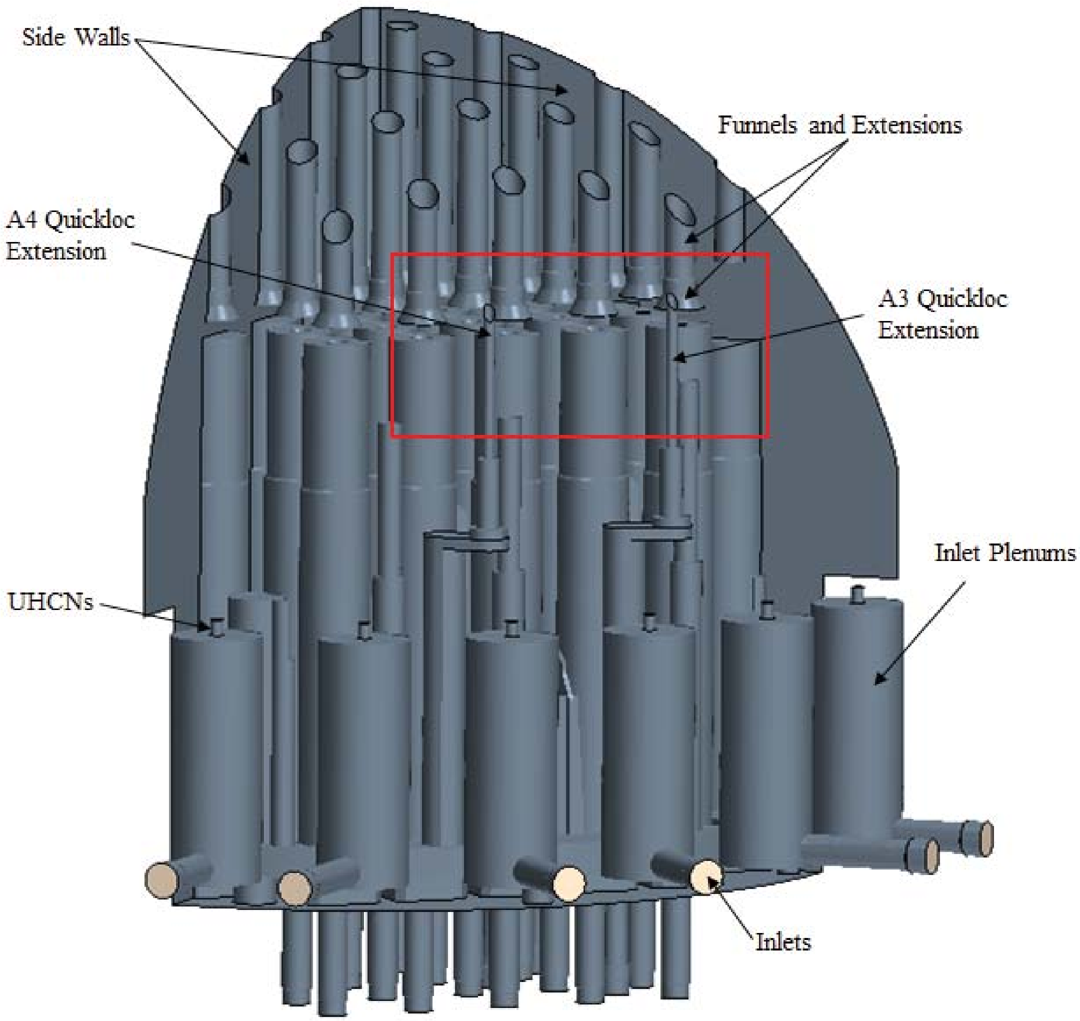

Figure 1 Geometry of the AP1000 ¼ Scale Upper Head Test

2. METHOD DISCUSSION

The purpose of this work was to be able to provide velocity information near certain components along with the associated uncertainty. Defined as:

$$CFD + E \pm u_{\mathrm{val}} \tag{1}$$

Where CFD is the result of the quantity of interest from the CFD analysis, E is the comparison error between the CFD and test data, and u_{val} is the uncertainty do to numerical, input and test data uncertainties. This work follows the methodology set forth in [1]. Because of the design cycle limitations combined with the complexity of the upper head geometry, a practical number of cases were run. This section will first briefly discuss the base case model, the sensitivity cases and the uncertainty methodology. The results will be discussed in Section 3.

2.1. Base Case Methodology

A solid model of the geometry, based on the test drawings, was used to create the mesh. Minor simplifications and improvements were made to the solid model as needed to aid in mesh development.

The mesh was developed in Star-CCM+6.02.009, and the base case mesh is on the order of 20,000,000 control volumes. The mesh type used is trim cell mesh in which most cells are of type hexahedral. Use of the trim cell mesh was based on experience gained from [4].

On all wall boundaries, prism layers were used in order to capture near wall effects. The initial cell height (for the wall layer) ranged from 0.005 inch to 0.0075 inch, while a geometric growth rate of 1.0 to 1.20 was used. The initial cell height was determined to be acceptable after running the model and observing the y^+ values. In general, the y^+ for the higher velocity areas (upper head wall) was below 400. Although not ideal, this provided the best compromise for runtime and mesh quality. For the most part, a total of five prism layers were used in most regions, with possible exception in the regions of narrow gaps. For surfaces and regions, a base element size of 0.1 inches was used for the base case. Once again, in regions where narrow gaps exist, adjustments to the default sizes were necessary. Figure 2 shows the base case mesh for the AP1000 ¼ scale upper head. It should be noted that regions of interest (i.e where data comparisons would be made) were meshed with a higher density mesh.

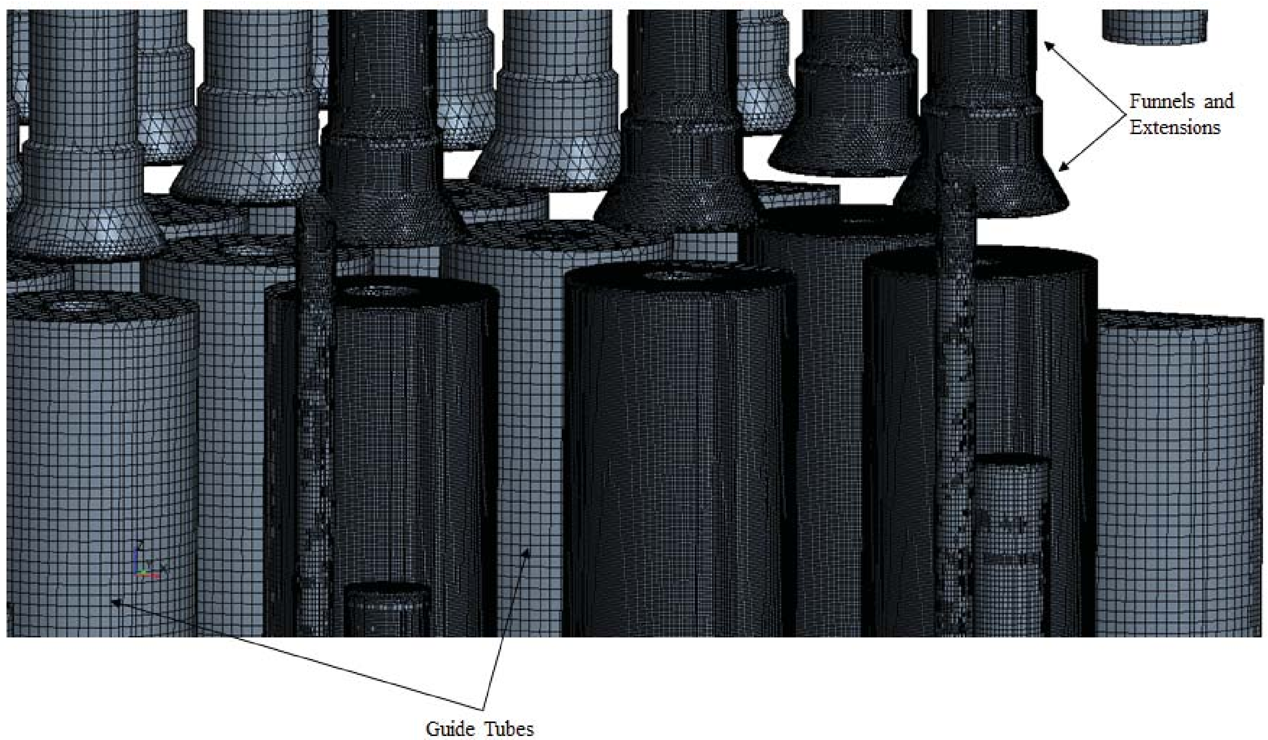

Figure 2 Surface Mesh Representation of AP1000 ¼ Scale Upper Head (Guide Tubes) (The red oval in Figure 1 shows the location)

Based on previous analyses, but also the inherent complex flow field, it was determined to run the model in a transient manner. Based on an estimated average advection time, the transient was run for 15 seconds.

The *k-ω* shear stress transport (SST) turbulence model was used, since it has the widest turbulence range of accuracy of the two-equation turbulence models present in Star-CCM+. The *k-ω* SST model is more accurate and reliable for a wider class of flows, like adverse pressure gradients in airfoils, transonic shock waves, etc. [3]. RANS modeling was chosen over a Large Eddy Simulation (LES) approach because of the large amount of mesh that would be required for this complex geometry and the associated computer run time that would be needed for LES. The RANS modeling provides a more economical approach for this application and is shown to provide conservative results for the quantities of interest.

2.2. Sensitivity Methodology

Prior to obtaining test data, various model sensitivities were performed, which were used in the uncertainty assessment. A summary of the different model sensitivities can be seen in Table I. All of these sensitivities are used as input to the calculation of u_{val} except for the turbulence sensitivity, which was used in the assessment of the test to CFD model error (E).

Table I. Summary of Model Sensitivities

Case Name	Sensitivity	Base Case Input	New Input
1.5X Base (35 Million Cells)	Cell Base Size Mesh	0.1 inch	0.075 inch
1.75X Base (55 Million Cells)	Cell Base Size Mesh	0.1 inch	0.06 inch
2X Base (84 Million Cells)	Cell Base Size Mesh	0.1 inch	0.050 inch
4X Base (239 Million Cells)	Cell Base Size Mesh	0.1 inch	0.035 inch
High y+	Near Wall Mesh	Two-layer, all y+, 5 layers	High y+, 3 wall layers
All y+	Near Wall Mesh	Two-layer, all y+, 5 layers	Two-layer, all y+, 15 layers
IC 1	Inlet Condition	I = 0.01, R = 10	I = 0.1, R = 10
IC 2	Inlet Condition	I = 0.01, R = 10	I = 0.01, R = 100
TS 1	Time Step	$\Delta t = 0.01s$	$\Delta t = 0.005s$
TS 2	Time Step	$\Delta t = 0.01s$	$\Delta t = 0.0025s$
IT 40	Transient	IT (Inner Iterations) = 20	IT (Inner Iterations) = 40
Runout	Transient	t = 15s	t = 20s
Realizable	Turbulence Model	$k - \omega$ SST	Realizable k - ε
Quadratic	Turbulence Model	$k - \omega$ SST	Standard $k - \varepsilon$ (quadratic relationship)
Full Scale	Test Set-up	Test Set-up	Test configuration at prototypic conditions
360°	Test Set-up	Test Set-up	Prototypic geometry @ ¼ scale geometry and flow
Notes: 1. The “Base Case” mesh has roughly 20 million cells.			

At the time the sensitivity runs were made, the locations of the test data were unknown, thus post-processing took place on several component iso-surfaces. In addition, each iso-surface was split into several elevations, where the maximum and surface average of the field mean were reported.

In Table I, each consecutively finer mesh was achieved by reducing the mesh base size. The model was re-meshed and a new solution was obtained. A base size of 0.035 inch was the smallest attainable due to the size of the model. The mesh refinements were used to determine the numerical uncertainty which is discussed in Section 3.2.1. For the near wall mesh sensitivity, the wall layer mesh was refined and coarsened. When the near wall mesh was coarsened, the wall treatment option was switched to the high y^+ option.

For the turbulence model sensitivities, two additional models were used. The realizable $k-\varepsilon$ is a variant of the standard $k-\varepsilon$ model, which is generally suited for wall bounded jets. The standard $k-\varepsilon$ (quadratic relationship) is more sophisticated than the standard $k-\varepsilon$ in that it uses a non-linear constitutive relationship. This takes into account flow anisotropy, which is inherent in 3-D, complex, turbulent flows.

The final sensitivities performed involve runs that took into account the differences between the test set up and the prototypic plant. Initially, the test configuration (i.e., ¼-symmetry) was scaled to prototypic scale, and run at prototypic conditions (i.e., flow rate, temperature, pressure, etc.). Then, the prototypic geometry (i.e., 360°, with prototypic features) was run at test conditions (i.e., ¼-scale and test flow rates). The purpose of these runs was to determine any sensitivity due to the test set-up (i.e. ¼-symmetry, side walls, etc), and also sensitivity due to a reduced Reynolds number.

The time step study shows that results do not change significantly when the transient solver settings are adjusted. Also, the model appears to be insensitive to inputs such as turbulent intensity (I) and dissipation ratio (R). The turbulence model sensitivity and the near wall mesh sensitivity will not be considered in the overall uncertainty term. This is due to the fact that the error in turbulence modeling will be accounted for while making comparisons to test data; thus accounted for in the value of E (Eq 1). It is expected that mesh sensitivity and test-setup sensitivity will have the largest effect on the overall uncertainty. For all sensitivities, the base case tends to return higher values of velocity. All sensitivities performed in this section will be taken into account to determine the overall validation uncertainty (u_{val}) of the model.

2.3. Uncertainty Methodology

An uncertainty analysis was performed based on input uncertainty, numerical uncertainty and test data uncertainty. The input uncertainty was computed by adjusting input parameters (i.e., turbulence intensity, dissipation ratio, etc.), and then re-running the analysis. Sensitivity coefficients were computed, and the resulting input uncertainty was obtained. A rigorous numerical (discretization) uncertainty was obtained via a least squares approach [2]. The test data uncertainty was provided with test data from ARL. The overall validation uncertainty can be obtained by taking the square root sum of the squares (SRSS) of each component. It should be noted, the final overall validation uncertainty is based on a 95% confidence interval.

$$u_{val} = \sqrt{u_{num}^2 + u_{inp}^2 + u_D^2} \quad (2)$$

Initially, the numerical discretization was determined using a standard Richardson extrapolation approach outlined in 2-4.1 of [1]. However, after an initial pass, it was determined that this approach did not produce reliable results for this case. This was due to the fact that monotonic convergence was not observed. For many complex, highly turbulent flow fields, this is the case. For situations like this, Eça and Hoekstra [2] developed a least squares method for determining an appropriate/realistic value of the predicted order of accuracy, p. In some instances, the value of p must be limited to the theoretical value, which in this case is 2. This needed to be done when super convergence was seen, (i.e. the order of accuracy higher than that of the code). In theory, the order of accuracy for most CFD codes is 2; however, some codes can achieve an order of accuracy close to 3, which can be done by employing higher order differencing schemes. The exact details of this approach can be seen in [2].

For the input uncertainty, certain input parameters (i.e., turbulent intensity, dissipation ratio, etc.) were altered, and the analyses were re-run. Since this benchmark was being performed on a scaled model test of a 90° sector of the upper head, it was appropriate to include an assessment of these in the uncertainty analysis. As such, the scale model to full scale uncertainty was included with the input uncertainties by running separate sensitivities on the Reynolds number and the 90° versus 360° geometries. It should be noted that uncertainties associated with scaling are not covered in ASME V&V 20 [1]. However, as described above, assessing it as an input uncertainty will determine the effects of scaling.

To assess the input uncertainties velocities were extracted from iso-surfaces, and the sensitivity due the altered inputs was assessed. The input uncertainty was taken from [1], and goes as:

$$u_{inp}^2 = \sum_{i=1}^{k} \left(\frac{\partial S}{\partial X_i} u_{x_i} \right)^2 \tag{3}$$

Where: S is the simulation result, X_i is the input parameter and u_{x_i} is the uncertainty in input X_i.

The partial differential can be approximated by a first order difference method, or:

$$\frac{\partial S}{\partial X_i} = \frac{S(X+\Delta X_i)-S(X_i)}{\Delta X_i} \tag{4}$$

In Equation 4, ΔX_i is the change in input variable from the nominal value, and $S(X_i)$ and $S(X + \Delta X_i)$ are the simulation results evaluated at the nominal input value and adjusted input value, respectively.

3. Analysis and Results

All analyses were carried out using Star-CCM+ 6.02.009. The field mean function was used in Star-CCM+ to store the time average at every control volume for selected variables. In this case, all three components of velocity were tracked, in addition to the cross flow velocity (magnitude of the horizontal components of velocity).

Data were processed in two general methods: 1) Time-averaged cross flow velocities were computed on component iso-surfaces; and 2) Time-averaged component velocities were extracted to coincide with LDV and PIV locations. Model sensitivities and resulting velocity uncertainties are based on cross flow velocities extracted at the iso-surfaces.

This section details the comparison of the CFD to the test data and calculation of the uncertainty.

3.1. Comparisons to Test Data

Comparisons between CFD results and selected test data will be presented in this section. The locations selected for comparison were taken based on significance. For example, downstream structural analysts consider the upper Quickloc location a region of interest; thus, these locations were considered. It should be noted that only three CFD models were compared to test data: 1) the base case 2) the mesh sensitivity case where the cell base size was set to 0.05 inch, and 3) the quadratic turbulence model case.

Comparisons between CFD and LDV data at the A4 Quickloc location can be seen in Figure 3. All three surveys shown in Figure 3 are parallel to A4 Quickloc (see Figure 1 for A4 location). Also, only the u_1 component is plotted, which runs parallel to the A4 rod (+ upward). As seen in the figure, all CFD cases compare fairly well to the test data. The base case CFD model ("CFD" in the legend) is favored because it overpredicts the test data. For downstream design analyses, higher velocities are not only conservative, but desireable.

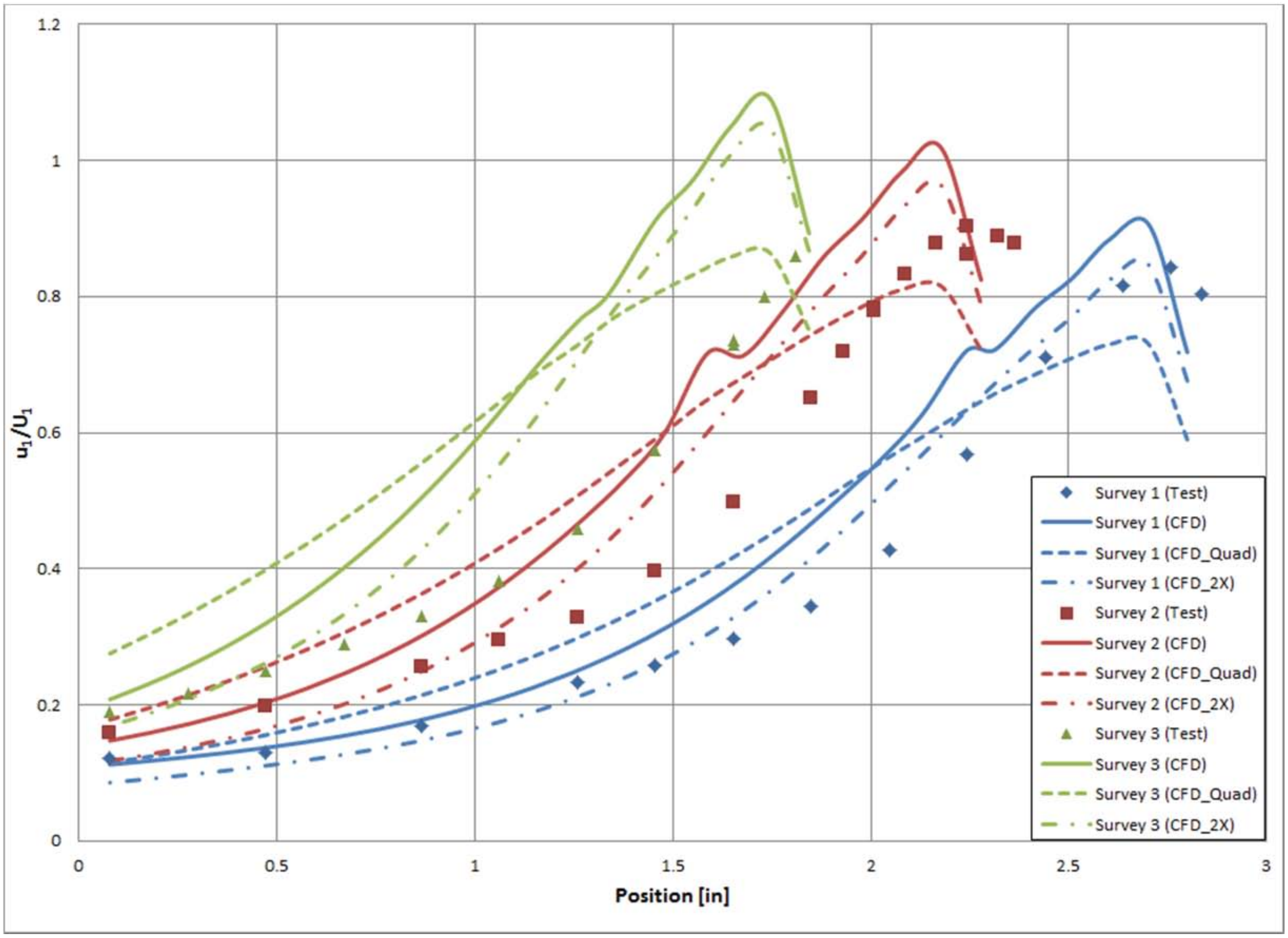

Figure 3 Normalized Mean Velocity Component near Quickloc Extensions

Comparisons to PIV data were performed in two different ways: 1) Vector contours for general/overall flow patterns; and 2) Detailed line plots for in-depth comparisons. Vector plots from test data and select CFD results at a location where PIV data was collected between the vessel head and a Quickloc are shown in Figure 4.

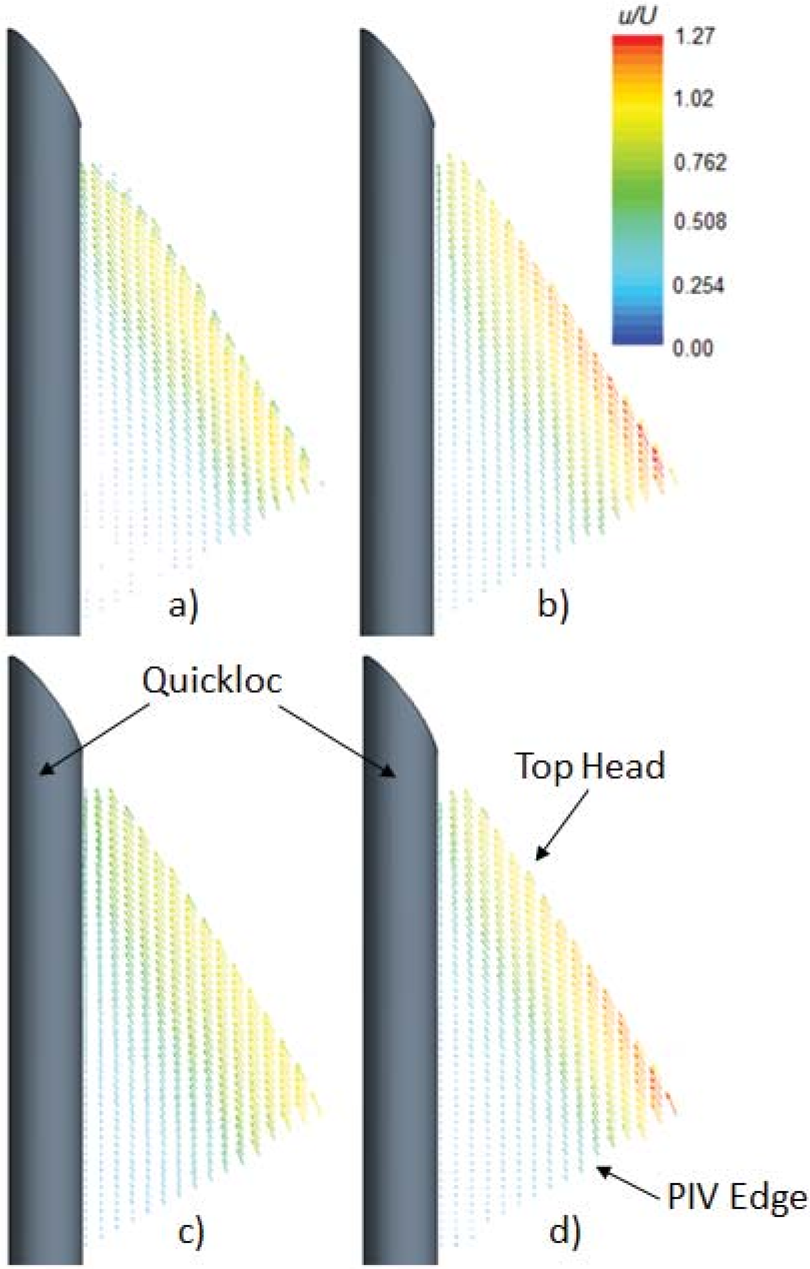

Figure 4 Quickloc PIV a) Test Data b) Base CFD Model c) Quad CFD Model d) 2X CFD Model

As seen from the figure, the overall flow pattern of the CFD model seems to agree with the test PIV data. The CFD results generally over predict the test, suggesting that in the CFD model cooling nozzle jet does not diffuse as quickly as was observed in the test. In general, higher velocity is considered conservative with respect to steady flow and turbulence related design purposes. Thus, from a design perspective an over prediction of velocity in this region is acceptable. A detailed look at the PIV data can be seen in Figures 5 and 6. These plots were created by extracting lines of data from the vessel head to the Quickloc.

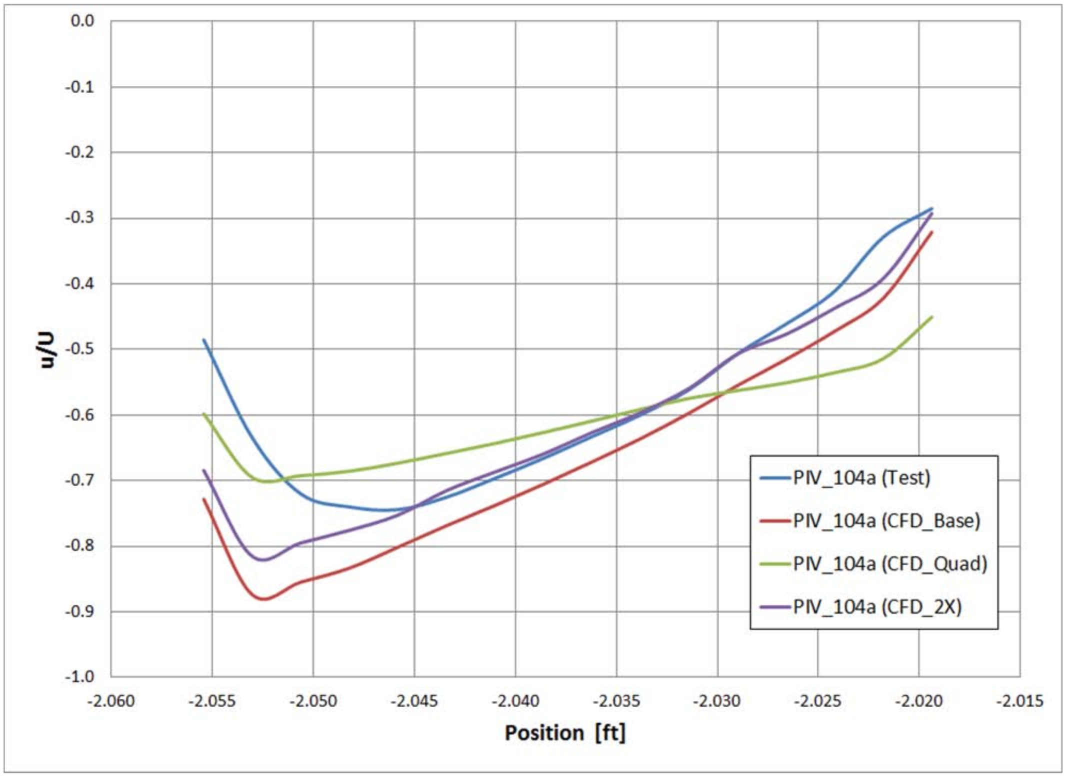

Figure 5 X-Component of Normalized Velocity for Select PIV Location

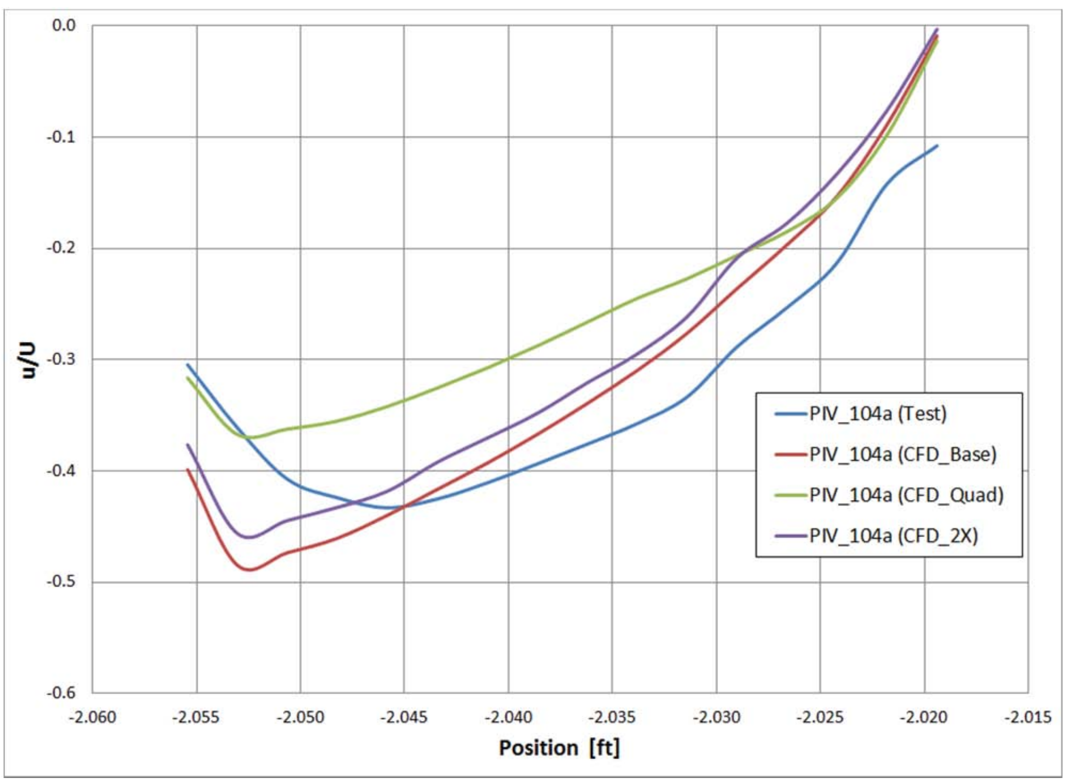

Figure 6 Y-Component of Normalized Velocity for Select PIV Location

Comparisons between the test data and CFD results are good reasonable. In general, the CFD results over predict the peaks for the x and y-components of velocity. The k-ε (Quadratic) model does not pick up the steep gradients at the vessel head.

The comparison error between the test data and CFD results can now be calculated. Since the CFD uncertainties (computed based on sensitivity runs) determined at iso-surface locations, it would make sense to compute the comparison error based on the test PIV sheets. From Equation 1-5-1 of [1], the comparison error E was calculated to be -18% based on the peak velocity.

3.2. Uncertainty Results

The results of the uncertainty approach outlined in section 2.3 will be presented in this section. As discussed earlier in this document, the results will be broken down by the following uncertainty components: 1) discretization uncertainty, 2) input uncertainty and 3) test data uncertainty.

3.2.1. Discretization Uncertainty

As discussed in Section 2.2, least squares method in [2] was used in determining the predicted order of accuracy. Five meshes were used to determine this uncertainty, which included the base mesh, 1.25X base mesh, 1.5X base mesh, 2X base mesh and 4X base mesh. The results of the mesh sensitivity runs can be seen in Figure 7. This figure shows the surface average of cross flow velocity at each component iso-surface. The surface of particular interest is 2c-iso-6, which is the upper portion of the Quickloc. As seen in the figure, for the most part, the base case model tends to return a larger value than subsequent finer meshes.

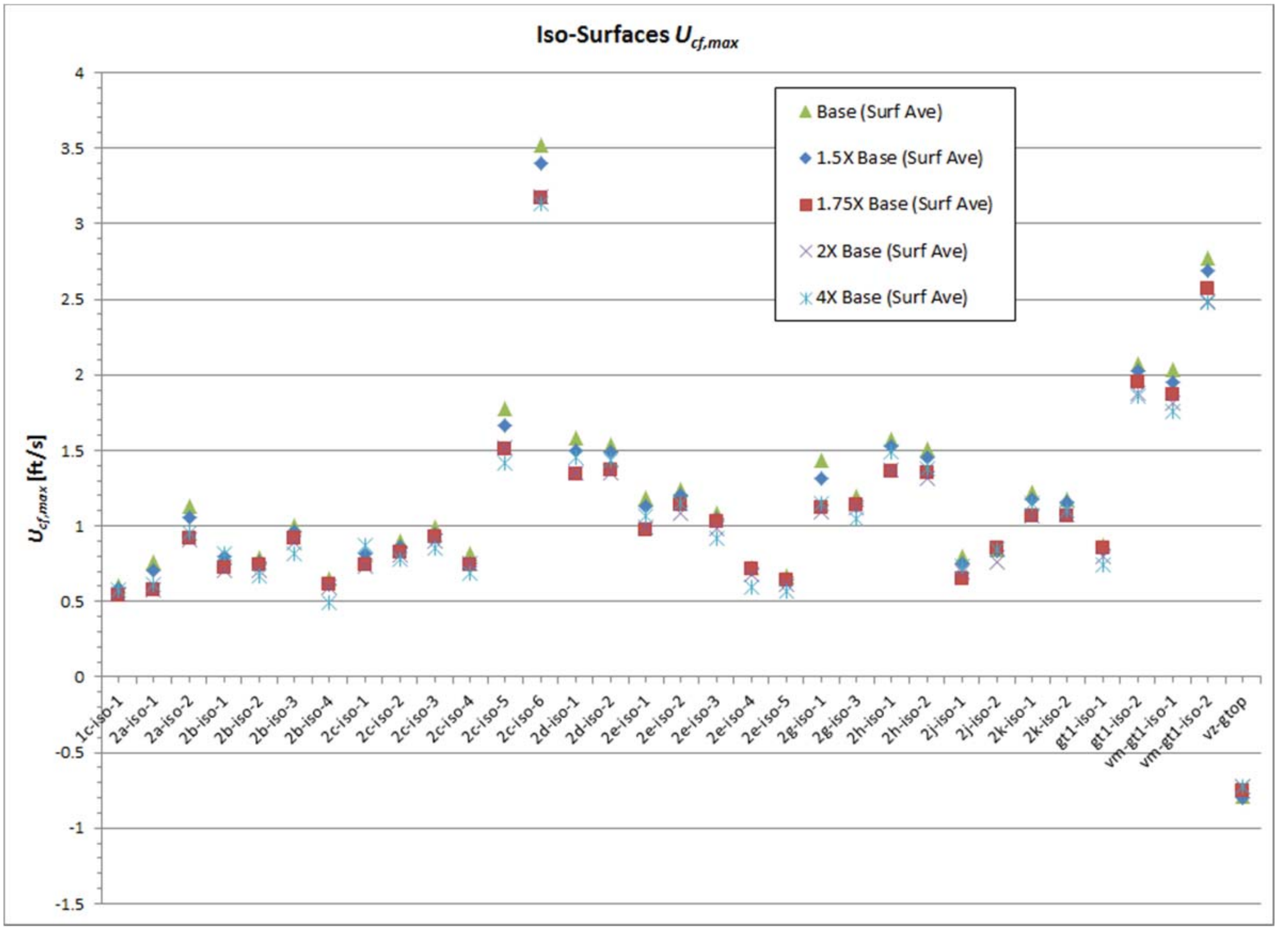

Figure 7 Mesh Sensitivity – Surface Average of the Field Mean of the Cross Flow Velocity

In the region near the Quickloc, a numerical uncertainty of roughly 25% was computed using the least squares approach. In the future, this may be able to be reduced by modifying the mesh and performing additional mesh sensitivity studies.

3.2.2. Input Uncertainty

The input uncertainty was determined for turbulence intensity, dissipation ratio, Reynolds number effect (i.e. scaled versus full scale) and geometry (i.e. 90° model versus 360° model). The velocities were extracted from the iso-surfaces; and the sensitivity, as a result of the altered input, was assessed. The input uncertainty was calculated from equation 4. Each input uncertainty was computed as based on this equation, and the total input uncertainty was arrived at by taking the SRSS of each component. The results for the base case, 360° case, and full scale case can be seen in Figure 8. The 360° case and the full scale case provide an assessment of the uncertainty do to extrapolation. As can be seen, most of this uncertainty was due to effects of the 90° versus 360° model. This implies in the full 360° geometry there are additional flow patterns that set up there are restricted in the 90° model. This is an important observation and should be considered more vigorously in the design of future benchmark test. Other inputs such as the dissipation ratio (*R*) and the turbulence intensity (*I*) have an insignificant effect on the overall result. Finally, Table II shows the input uncertainties in the region of the Quickloc. These uncertainties result in a u_{inp} of roughly 11% was computed.

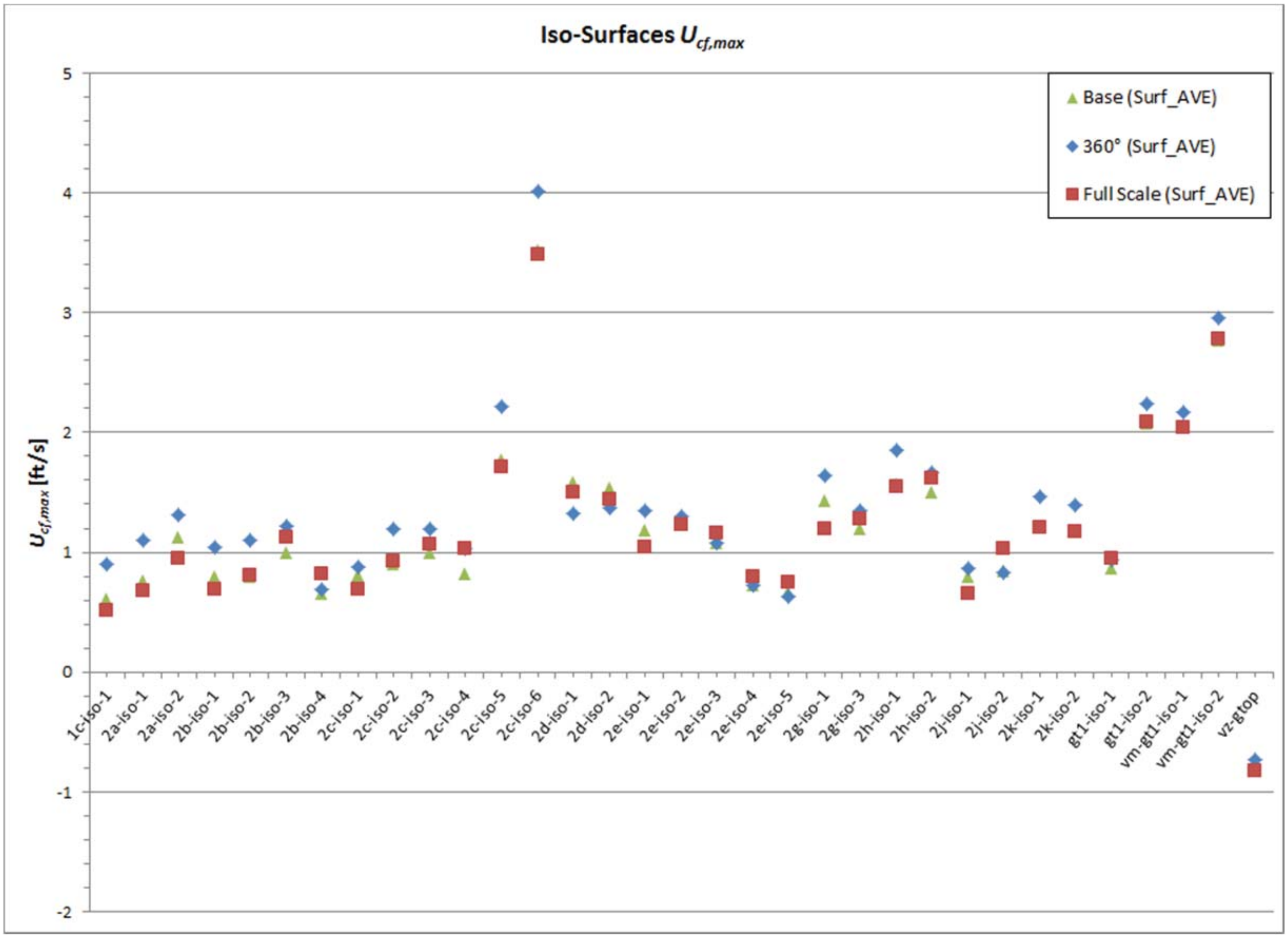

Figure 8 Input Sensitivity – Base, Full Scale & 360° Models

Table II. Input Uncertainties in the Quickloc region

Region	$u_{inp,I}$ [%]	$u_{inp,R}$ [%]	$u_{inp,Re}$ [%]	u_{360} [%]
Upper Quickloc	0.0949	0.269	0.733	6.87

3.2.3. Test Data Uncertainty

In general, the experimental uncertainty is broken down into two parts: 1) the systematic uncertainty, and 2) the random uncertainty. The total experimental uncertainty (u_D) is the SRSS of both components. Since the region of interest for the test measurements and resulting CFD calculations is the upper Quickloc region, it was appropriate to use PIV data nearest the Quickloc. A test data uncertainty (u_D) of roughly 20% was observed.

4. CONCLUSIONS

In conclusion, the CFD base case compared fairly well to the test data. An overall validation uncertainty of 34% was computed using Equation (2), while the error (*E*) computed in Section 3.1 was roughly -18%. It should be noted that the discretization uncertainty, the test data uncertainty, and the uncertainty associated with the 90° versus 360° model (i.e. part of the extrapolation to full scale) are the major contributors to the overall validation uncertainty.

CFD - 18% +/- 34%

As seen in results, the base case model tends to over predict the test data. Due to the inherent unsteadiness of this complex flow field, an unsteady Reynolds Averaged Navier-Stokes (RANS) was used, along with the $k - \omega$ SST turbulence model. This turbulence model predicted the test data well, as compared to other turbulence models. However, as turbulence modeling is an area of ongoing research, it is suggested that in the future, new turbulence models could be considered if that would provide even better representation of the results.

REFERENCES

1. ASME V&V 20-2009, "Standard for Verification and Validation in Computational Fluid Dynamics and Heat Transfer," November 30, 2009.
2. Luís Eça and Martin Hoekstra, "Discretization Uncertainty Estimation based on a Least Squares version of the Grid Convergence Index," 2nd Workshop on CFD Uncertainty Analysis, October 2006.
3. F.R. Mentor, M. Kuntz and R. Langtry, "Ten Years of Industrial Experience with the SST Turbulence Model," Turbulence, Heat and Mass Transfer, 2003.
4. M-T Kao, et.al., "CFD Analysis of PWR Reactor Vessel Upper Plenum Sections – Flow Simulations in Control Rod Guide Tubes," Proc. 18th Int. Conf. on Nuclear Engineering, Paper No. ICONE 18-29466.